665. Dynamic response of an embedded railway track subjected to a moving load

J. H. Zou, W. X. Feng, H. B. Jiang
Faculty of Civil and Transportation Civil Engineering, Guangdong University of Technology
Guangzhou 510006, China
E-mail: *zoujinhua@gdut.edu.cn*

(Received 12 June 2011; accepted 5 September 2011)

Abstract. A dynamic computational model for the embedded railway track subjected to a moving load is developed in this paper. The model consists of two-layer Euler-Bernoulli beams and continuous viscoelastic elements. The lower beam, the upper beam are employed to model the concrete slab and the rail, respectively, whilst the continuous viscoelastic elements model the soil reaction and the fill material. The problem is solved by employing Newmark-β numerical integration method. The effects of the speed of the moving loads, the rail type, and the spring stiffness of rail supports are studied. Results indicate that the dynamic response of rail and slab increases with the larger moving load speeds, whilst the response of rail and slab decreases with the increase of spring stiffness and heavier rail used.

Keywords: embedded railway track, finite element method, moving load, dynamic response.

Introduction

The application of concrete non-ballasted track in urban railway transportation has certain advantages compared with conventional ballasted track, but existing concrete non-ballasted track structures produce more vibration and noise than ballasted track. For this reason, a "silent slab track" developed in the Netherlands is shown in Fig. 1. The structure consists of a massive concrete slab, into which the rails are embedded by means of Corkelast material [1 - 3]. And unlike older rail systems, the rail track is continuously welded, which can result in a smoother and quieter ride.

To efficient design such as an embedded track, it is necessary to gain the specific features of the dynamic behavior of the structure. This can be accomplished with a simple analysis of the structure model taking into account the main physical characteristics of the real structure [4].

In this paper, we model the embedded track as two elastic Euler-Bernoulli beams and continuous viscoelastic elements (Fig. 2). As the structure is symmetrical, we can analyze only half of it. The upper beam models the rail, whilst the lower one represents the concrete slab. The viscoelastic elements that connect them represent the fill materials. The viscoelastic elements that support the lower beam models the subsoil reaction. The point load moving at a constant speed v is representative of the usual wheel load, currently used in the analysis and design of railway track. The dynamic equilibrium equations of motions of finite element form for the track system are derived by means of the principle of Lagrange's equation [5] and these equations are solved by the Newmark-β step-by-step integration method to obtain the dynamic responses of the track system.

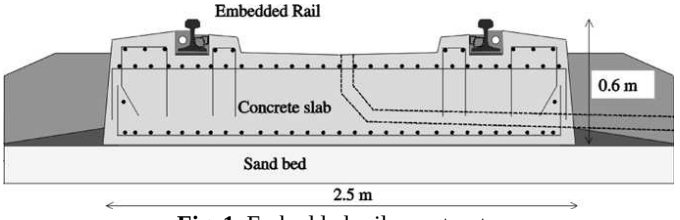

Fig. 1. Embedded railway structure

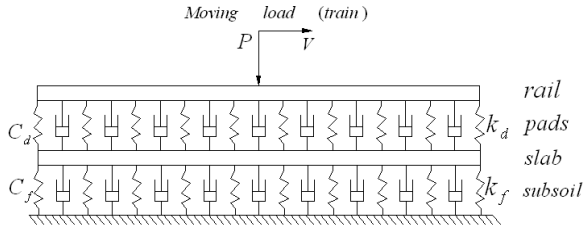

Fig. 2. The model for an embedded railway track

Analysis based on a finite element model

Finite element method is employed to establish the dynamic equation of the embedded railway track, where rail and concrete slab as beams with finite length are discretized as two-dimensional beam elements.

Element stiffness matrix

Consider a generalized beam element ij of length l of two beams on continuous viscoelastic foundation as shown in Fig. 3, which is assumed that the downward deflections of the element are taken as positive and that they are measured with reference to their respective vertical static equilibrium positions. Neglecting the longitudinal displacements, the element has four degrees of freedom per node, the transverse displacements and the rotations of the upper and lower beam, respectively, and thus possesses a total of 8 degrees of freedom. The element nodal displacements are given by:

$$\{\delta\}_i^{(e)} = \left[w_i \quad \theta_i \quad w_i^* \quad \theta_i^* \quad w_j \quad \theta_j \quad w_j^* \quad \theta_j^*\right]^{(e)T} \tag{1}$$

where asterisk denotes the displacements of the lower beam of the element. The transverse displacements w of the beams are expressed in the nodal displacements by Hermitian cubic interpolation functions:

$$w_1 = [N_1]\{\delta^{(e)}\},\ \theta_1 = [N_1]\{\delta^{(e)}\},\ w_2 = [N_2]\{\delta^{(e)}\},\ \theta_2 = [N_2]\{\delta^{(e)}\} \tag{2}$$

where:

$$[N_1] = [N_{i1} \quad N_{i2} \quad 0 \quad 0 \quad N_{i3} \quad N_{i4} \quad 0 \quad 0]$$

$$[N_2] = [0 \quad 0 \quad N_{i1} \quad N_{i2} \quad 0 \quad 0 \quad N_{i3} \quad N_{i4}]$$

$$N_{i1} = 1 - 3(x/l)^2 + 2(x/l)^3,\ N_{i2} = x - 2x^2/l + x^3/l^2$$

$$N_{i3} = 3(x/l)^2 - 2(x/l)^3,\ N_{i4} = -x^2/l + x^3/l^2$$

w_1 and w_2 are the vertical displacements of the upper beam and the lower beam, respectively. x is local coordinate measured from the left node of the element.

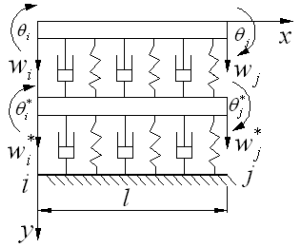

Fig. 3. A generalized beam element for the track structure

For the generalized beam element, the elastic strain energy consists of the strain energy of the upper beam and the strain energy of the lower beam of the element, the strain energy of the continuous viscoelastic elements between the upper beam and the lower beam of the element, the strain energy due to the foundation stiffness:

$$\frac{1}{2}\int_0^l E_r I_r (\frac{\partial^2 w_1}{\partial x^2})^2 dx + \frac{1}{2}\int_0^l E_c I_c (\frac{\partial^2 w_2}{\partial x^2})^2 + \frac{1}{2}\int_0^l k_d (w_1 - w_2)^2 dx + \frac{1}{2}\int_0^l k_f w_2^2 dx$$
$$= \frac{1}{2}\{\delta\}_i^{(e)T}([K]_r^{(e)} + [K]_c^{(e)} + [K]_d^{(e)} + [K]_f^{(e)})\{\delta\}_i^{(e)} \quad (3)$$

where:

$$[K]_r^{(e)} = E_r I_r \int_0^l [N_1]''^T [N_1]'' dx, \quad [K]_c^{(e)} = E_c I_c \int_0^l [N_2]''^T [N_2]'' dx$$

$$[K]_d^{(e)} = k_d (\int_0^l [N_1]^T [N_1] dx - \int_0^l [N_1]^T [N_2] dx - \int_0^l [N_2]^T [N_1] dx + \int_0^l [N_2]^T [N_2] dx$$

$$[K]_f^{(e)} = k_f \int_0^l [N_2]^T [N_2] dx$$

In which, E_r and E_c - Young's module of the upper rail beam and the lower concrete beam, respectively, I_r and I_c - moment of inertia of the upper two rails beam and the lower concrete slab, respectively, k_d - stiffness of the fill material, k_f - stiffness of the foundation.

Finally, using Lagrange's equations, the (8×8) complete stiffness matrix for the element can be expressed as:

$$[K]^{(e)} = [K]_r^{(e)} + [K]_c^{(e)} + [K]_d^{(e)} + [K]_f^{(e)} \quad (4)$$

Element mass matrix

For dynamic analysis, it is necessary to derive the element mass matrix. In this paper, the mass matrix is derived by considering the kinetic energy due to lateral velocity of the element. This is consistent with the derivation of the stiffness matrix. The kinetic energy of the generalized beam element shown in Fig.3 is given by:

$$T = \frac{1}{2}\int_0^l \overline{m}_r (\frac{\partial w_1}{\partial t})^2 dx + \frac{1}{2}\int_0^l \overline{m}_c (\frac{\partial w_2}{\partial t})^2 dx \quad (5)$$

where $\overline{m}_r$ and $\overline{m}_c$ are the mass densities of the upper rails beam and the lower concrete beam per length, respectively.

Using Lagrange's equation, on the kinetic energy term above, the element mass matrix $[M]_l^e$ is given by:

$$[M]^{(e)} = [M]_r^{(e)} + [M]_c^{(e)} \quad (6)$$

where:

$$[M]_r^{(e)} = \overline{m}_r \int_0^l [N_1]^T [N_1] dx, \quad [M]_c^{(e)} = \overline{m}_c \int_0^l [N_2]^T [N_2] dx$$

Element damping matrix

The potential energy of the damping force of the generalized beam element is comprised of the potential energy of the damping force of the upper beam and the lower beam, the potential energy of the damping force of the continuous damping elements between the upper beam and the lower one as well as the potential energy of the foundation. For the embedded track system, Rayleigh damping is adopted. Conventionally, the structural damping has been computed on the structure level. Based on the definition of Rayleigh damping, the structural damping of the element is computed as follows:

$$[C]^e = \alpha([M]_r^{(e)} + [M]_c^{(e)}) + \beta([K]_r^{(e)} + [K]_c^{(e)}) \tag{7}$$

Given the damping ratio ξ, the two coefficients α and β can be determined as $\alpha = 2\xi\omega_1\omega_2/(\omega_1 + \omega_2)$, $\beta = 2\xi/(\omega_1 + \omega_2)$, where ω_1 and ω_2 are the first two frequencies of vibration of the track system.

The potential energy of the damping force of the continuous damping elements between the upper beam and the lower beam and the potential energy of the foundation are given by:

$$\begin{aligned}
&\int_0^l c_d \left(\frac{\partial w_1}{\partial t} - \frac{\partial w_2}{\partial t}\right)(w_1 - w_2) dx + \int_0^l c_f \left(\frac{\partial w_2}{\partial t}\right) w_2 dx \\
&= \int_0^l c_d ([N_1]\{\dot{\delta}\}_i^{(e)} - [N_2]\{\dot{\delta}\}_i^{(e)})([N_1]\{\delta\}_i^{(e)} - [N_2]\{\delta\}_i^{(e)}) dx \\
&+ \int_0^l c_f ([N_2]\{\dot{\delta}\}_i^{(e)})([N_2]\{\delta\}_i^{(e)}) dx \\
&= \{\dot{\delta}\}_i^{(e)T} [C]_d^{(e)} \{\dot{\delta}\}_i^{(e)} + \{\dot{\delta}\}_i^{(e)T} [C]_f^{(e)} \{\delta\}_i^{(e)}
\end{aligned} \tag{8}$$

where the dot represents differentiation with respect to time t. Using Lagrange's equations, $[C]_d^{(e)}$ and $[C]_f^{(e)}$ are given by:

$$[C]_d^{(e)} = c_d \left(\int_0^l [N_1]^T [N_1] dx - \int_0^l [N_1]^T [N_2] dx - \int_0^l [N_2]^T [N_1] dx + \int_0^l [N_2]^T [N_2] dx \right) \tag{9}$$

$$[C]_f^{(e)} = c_f \left(\int_0^l [N_2]^T [N_2] dx \right) \tag{10}$$

Thus, the (8×8) complete damping matrix for the generalized beam element can be expressed as:

$$[C]^e = \alpha([M]_r^{(e)} + [M]_c^{(e)}) + \beta([K]_r^{(e)} + [K]_c^{(e)}) + [C]_d^e + [C]_f^e \tag{11}$$

© VIBROENGINEERING. JOURNAL OF VIBROENGINEERING. SEPTEMBER 2011. VOLUME 13, ISSUE 3. ISSN 1392-8716

Dynamic equations of the embedded railway track

Consider a moving concentrated force proceeding with velocity v along the upper rail beam as presented in Fig. 3. The track has been divided into a number of finite elements. The dynamic equation for the model can be written as:

$$[M]\{\ddot{q}\}+[C]\{\dot{q}\}+[K]\{q\}=\sum[N]^T P \tag{12}$$

where:

$$[M]=\sum_e[M]_l^e,\ [C]=\sum_e[C]^e,\ [K]=\sum_e[K]_l^e \tag{13}$$

These are the structure mass matrix, the damping matrix and the stiffness matrix, and $\{q\}$, $\{\dot{q}\}$ and $\{\ddot{q}\}$ denote the displacement, velocity and acceleration vectors of the track structure, respectively. $[N]^T$ is a vector with zero entries except for those corresponding to the nodes of the element on which the load is acting [3], and P is the magnitude of the concentrated force.

In equation (12), the $[N]$ can be represented as:

$$[N]=[0\ \ ...\ \ N_{i1}\ \ N_{i2}\ \ 0\ \ 0\ \ N_{i3}\ \ N_{i4}\ \ 0\ \ 0\ \ ...\ \ 0] \tag{14}$$

where N_{i1}, N_{i2}, N_{i3}, N_{i4} are the same as the above equation (2), in which i is the number of elements on which the load is acting.

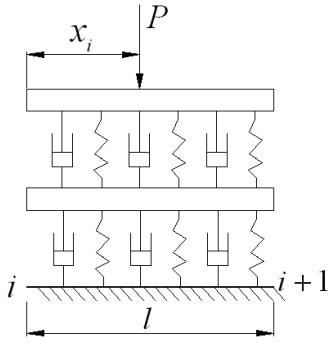

Fig. 4. Position of *P* at *t* time

The *Newmark-β* method of direct step-by-step integration is employed in the study to solve the dynamic equation (12) and the numerical procedure is implemented in a Fortran 90 program.

Numerical examples and discussion

In this section, the numerical simulation of an embedded railway track is performed based on the above analysis, and the effects of some parameters are investigated.

The effects of the speed of the moving load and rail type

To validate the method, the track structure of length 50 m subjected to a moving train axle load with constant velocity v is analyzed. The same material properties, spring and damping coefficients are adopted from concrete slab track of Ref.[6]: E_r = 2.06×1011 N/m^2, E_c = 2.1×10^{10} N/m^2, k_d = 6.0×10^7 N/m, c_d = 7.5×10^4 N•s/m, k_f = 6.25×10^7 N/m, c_f = 8.3×10^4 N•s/m, $\overline{m}_c$ =

557.81 kg/m. The element length is 1.0 m and the moving train axle load $P = 112800N$ is applied at the model. For *UIC50*, *UIC60* and *UIC75* rail type, the $\overline{m}_r$ and I_r are 51.514 kg/m and 2.037×10^{-5} m^4, 60.64 kg/m and 3.217×10^{-5} m^4, 74.414 kg/m and 4.489×10^{-5} m^4, respectively. The velocity of the moving load is varied from 15 m/s to 100 m/s.

The results for the dynamic influence in mid-span deflection are listed in Table 1. It is interesting to note that the deflections remain more and less constant for various moving speed, within the same rail type considered. However, the deflection increases slightly with moving speed. The maximum dynamic deflection can be observed at a speed of 100m/s. Hence, when the rail type is same, the influence of the moving load speed, in the range 15-100m/s, is quite insignificant as listed by the results. And we can also observe that the heavier rail can decrease the maximum deflections of rail and slab.

The effects of spring stiffness of rail supports

In order to analyze the dynamic response of the embedded railway track of spring stiffness of rail supports, the parameters are the same as the above, but the load travels with a constant velocity of v = 50 m/s. The spring stiffness of rail supports is varied from 3.0×10^7 N/m^2 to 1.2×10^8 N/m^2. This range covers the typical values in railway tracks of China. The maximum deflections of the rail and slab are calculated and listed in Table 2. It can be noted that when k_d and the rail type are increased, the deflections of both the rail and the slab decrease. Figs. 5-7 provide the time histories of the mid-span deflections of the rail and slab correspondingly. These results indicate that the dynamic deflections are greatly influenced by the spring stiffness of rail supports uniformly. And the deflections of rail and slab decrease when the heavier rail type is used.

Table 1. Maximum deflections of rail and slab of the embedded railway track: $w(\times10^{-4}m)$

Load velocity(m/s):	*UIC50*		*UIC60*		*UIC75*	
	rail	slab	rail	slab	rail	slab
0	6.29612	1.60122	5.54578	1.30006	4.96495	1.19302
15	6.29619	1.60131	5.54586	1.30008	4.96504	1.19305
30	6.29619	1.60228	5.54586	1.30008	4.96817	1.19376
50	6.34342	1.60229	5.60809	1.30014	4.96817	1.19376
70	6.34606	1.60230	5.61139	1.30026	4.96831	1.19401
85	6.34657	1.60235	5.61171	1.30043	4.96846	1.19401
100	6.34690	1.60235	5.61175	1.30043	4.96854	1.19408

Table 2. Maximum deflections of rail and slab of the embedded railway track: $w(\times10^{-4}m)$

Spring stiffness k_d	*UIC50*		*UIC60*		*UIC75*	
	rail	slab	rail	slab	rail	slab
3.0×10^7	10.40464	3.18957	8.69427	2.37717	7.39667	1.81682
6.0×10^7	6.34342	1.60229	5.60809	1.30014	4.96817	1.19376
1.2×10^8	4.01657	0.96760	3.68588	0.94598	3.44392	0.92879

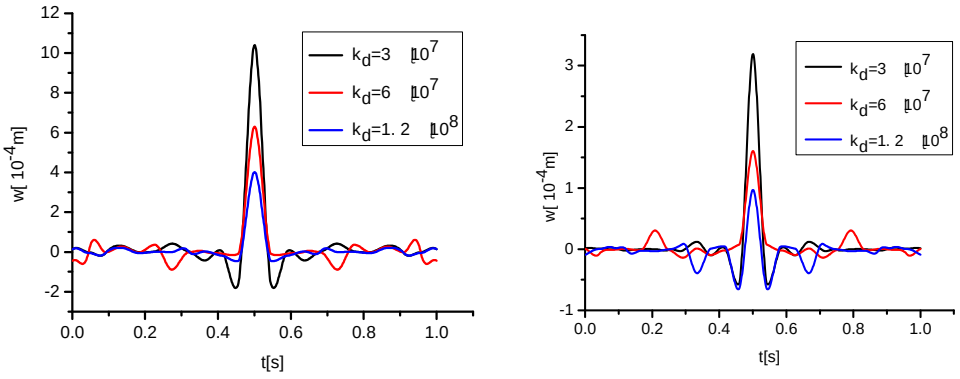

(a) the rail (b) the slab

Fig. 5. Time histories of midpoint deflection due to spring stiffness of rail supports for *UIC50*, *V=50m/s*

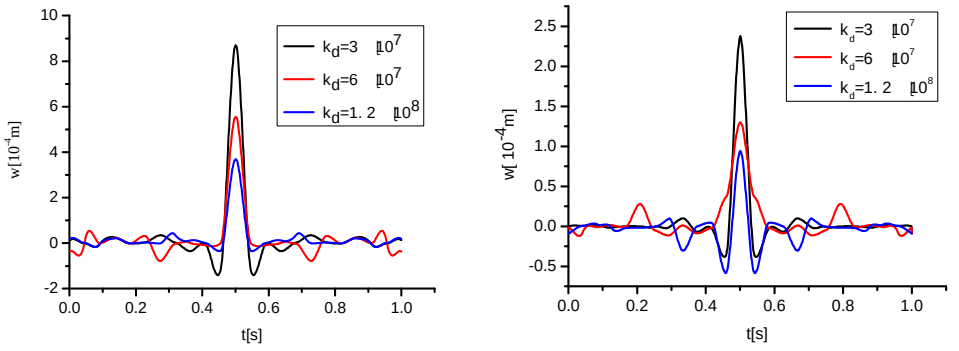

(a) the rail (b) the slab

Fig. 6. Time histories of midpoint deflection due to spring stiffness of rail supports for *UIC60*, *V=50m/s*

Conclusions

The study presented a dynamic finite element model for an embedded track to a moving load that represents the axle load of a train. The model is composed of two Euler-Bernoulli beams and continuous viscoelastic elements. The upper beam models the rail, whilst the lower one models the concrete slab. The viscoelastic elements that connect the upper beam and the lower one represent the fill material. The viscoelastic elements that support the concrete slab model the subsoil reaction. Hermitian cubic functions are utilized as the shape functions of the two-node generalized beam element of the track structure. The element stiffness, mass, damping matrix and element force vector can be obtained by Lagrange's equation. The equations are solved by Newmark–β integration method. The effects of some important parameters, such as the rail type, the moving speed, the spring stiffness of rail supports and the time histories of mid-span deflection, have been studied. From the presented analysis it is obvious that, when other parameters are kept the same, with the increase of load velocity, the dynamic response of rail and slab will increase. Meanwhile, with the heavier rail type and the increase of the rail support spring stiffness, the dynamic response of rail and slab will both decrease.

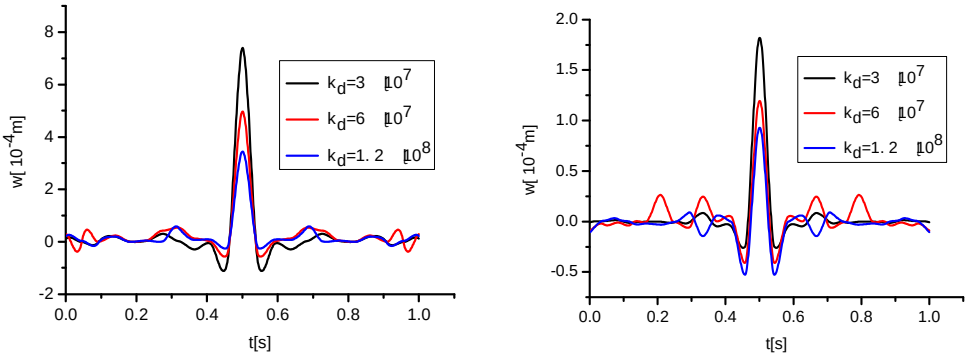

(a) the rail (b) the slab

Fig. 7. Time histories of midpoint deflection due to spring stiffness of rail supports for *UIC75*, *V=50m/s*

Finally, it should be pointed out that the dynamic response of the embedded railway track under a moving train is a very complicated problem. The results and conclusions obtained in this paper are preliminary, and studies on this field are still in progress. Because of the lack of calculation parameters of the track structure, we have adopted the parameters of slab track characteristic to railways in China.

Acknowledgement

This work reported herein is part of a project supported by the Foundation of the National Science of China under the project number 50378040. This support is gratefully acknowledged.

References

[1] Esveld C. Modern Railway Track. Netherlands: MRT Productions, 2001.

[2] Van Lier S. The vibro-acoustic modeling of slab track with embedded rails. Journal of Sound and Vibration, Vol. 231, 2000, p. 805-817.

[3] Shamalta M., Metrikine A. V. Analysis study of the dynamic response of an embedded railway track to a moving load. Archive of Applied Mechanics, Vol. 73, 2003, p. 131-146.

[4] Lin Y. H., Trethewey M. W. Finite element analysis of elastic beams subjected to moving dynamic loads. Journal of Sound and Vibration, Vol. 136, 1996, p. 323-342.

[5] Bathe K. J., Wilson E. L. Numerical Methods in Finite Element Analysis. Prentice-Hall: Englewood Cliffs, N. J., 1976.

[6] Lou P., Zeng Q. Y. Finite element analysis of slab track subjected to moving load. Journal of Traffic and Transportation Engineering, Vol. 4, Issue 1, 2004, p. 29-33.